

Optically Amended Biosynthesized Crystalline Copper-Doped ZnO for Enhanced Antibacterial Activity

Adam Mengistu ^a, Mohammed Naimuddin ^{*a}, Buzuayehu Abebe ^{*b}

^aDepartment of Applied Biology, School of Applied Natural Science, Adama Science and Technology University, Adama, P.O. Box:1888, Ethiopia.

^bDepartment of Applied Chemistry, School of Applied Natural Science, Adama Science and Technology University, Adama, P.O. Box:1888, Ethiopia.

Experimental

1. Collection of Plant

Fresh leaves of *Solanum incanum* that weigh about 1 kg were collected from the field. Just after the collection of plant material, it was brought to the laboratory and washed thoroughly with fresh water and then washed with distilled water. The cleaned plant material was allowed to air dry in the lab at 25 °C, crushed manually, and ground by an electric grinder to get a fine-textured powder. The powder was then sieved through a mesh to get particles of uniform size, and 234 g was stored in the refrigerator in a polymeric plastic bag.

2. Preparation of the Plant Extract

The aqueous extract of the plant was prepared by cold maceration. For this purpose, 50 g of powdered plant leaf was soaked in 500 mL of distilled water, and the suspension was placed in a shaker at 25 °C for 24 h with continuous agitation at 120 rpm. The extract was filtered by Whatman filter paper #1 and stored at 4 °C for further analysis ¹.

3. Phytochemical Analysis

3.1. Test for Alkaloids

1 mL of the *S. incanum* extract filtrate was treated with 2-3 drops of Wagner reagent, and a yellow color formation was observed ².

3.2. Test for Flavonoids

The plant extract (2 mL) was mixed with a few fragments of magnesium ribbon, and 5% concentrated HCl was added dropwise. The appearance of pink scarlet has been looked at after 2 min to indicate the presence and absence of flavonoids ³.

3.3. Test for Phenols

1 mL of the plant extract filtrate was taken in a test tube, and 1 to 2 drops of iron III chlorides (FeCl₃) were added. The color change of the mixture was observed after a few min ⁴.

3.4. Test for Saponins

The filtrate of plant extract (1 mL) was taken in a test tube and diluted with 5 mL of distilled water. It was shaken by hand for 15 min. A foam layer was observed on the top of the test tube. This foam layer indicated the presence of saponins ³.

3.5. Test for Steroids

The plant extract filtrate (1 mL) was taken in a test tube and dissolved in chloroform (1 mL). Then 1 mL of acetic anhydride and 2 drops of concentrated sulfuric acid were added to the test tube by the sides. The upper layer in the test tube turned red, indicating the presence of steroids ⁵.

3.6. Tannins Test

The plant extract filtrate (2 mL) was taken, and then a few drops of 10% ferric chloride solution were added to the filtrate. The blue-green color appearance indicates the presence of tannins in the sample ⁴.

3.7. Terpenoids Test

The plant extract filtrate (1 mL) was taken in a test tube and dissolved in chloroform (1 mL). The concentrated sulfuric acid (2 drops) was added to the test tube and shaken. The lower yellow color indicates the presence of terpenoids ⁶.

4. Optimization of Synthesis Parameters

Aqueous solutions (0.25 M) of the precursor salts, i.e., zinc nitrate and copper acetate, were prepared. Three parameters, such as volume ratio (salt solution: plant filtrate), temperature, and the pH of synthesis, were used to optimize NPs synthesis. Since ZnO NPs were considered the host NPs, the optimization in the current study focused on Zn. The volume ratio optimization was carried out using leaves extract volumes of 10 and 20 mL, which were added dropwise to prepare a fixed zinc nitrate salt solution of 10 mL by continuous stirring at 80 rpm for 1.5 h using a magnetic stirrer at room temperature. Also, by varying the volume of solution (20, 30, and 40 mL) to the fixed amount of leaves extract (10 mL), the best ratio (2:1) out of five synthesis experiments for other parameters was selected (Table S1). Visual observation of brownish color was the indication of NPs formation. In addition, the formation of NPs was confirmed by measuring absorbance using a UV-visible spectrophotometer. Then, lastly, the optimally synthesized nanoparticle suspensions were centrifuged at 5,000 rpm for 30 min. The supernatant was discarded, and the pellet containing nanoparticles was washed

three times with deionized water and ethanol (96), and air dried in an oven. The ZnO NPs were stored in a cool, dry place for further analysis after calcined at a specific temperature ⁷.

Characterizations

An X-ray diffractometer (DW-XRD-Y7000, DRAWELL, China) was used to study the crystallinity, average crystallite size of ZnO and GCD-Z NCs, and Cu doping behavior. The particle size, crystallinity, and CuO-ZnO heterojunction were further confirmed by the TEM/HRTEM/SAED techniques (JEOL JEM 2100 HRTEM, JEOL, USA). Field emission scanning electron microscopy (FE-SEM, ZEISS SIGMA VP, Germany) was used to examine the material shape, elemental composition, and elemental mapping. The material's optical characteristics and energy bandgap were evaluated using a double-beam UV-vis P9 spectrophotometer (Carry 100 UV-Vis, Agilent Technologies, USA). By photoluminescence spectroscopy (S/N: MY18490002, Agilent Technologies, USA, at the scan rate of 600 nm/min) and laser excitation wavelength of 325 nm, additional optical properties, such as electron-hole recombination behaviours of ZnO NPs and GCD-Z NCs, were characterized. FTIR (FT/IR-6600typeA, JASCO Japan), at 2 mm/sec scanning speed, and detector TGS were used to study the chemical bonding and stiffness behaviors of ZnO NPs and GCD-ZNCs NCs before and after calcination.

Supplementary Figures

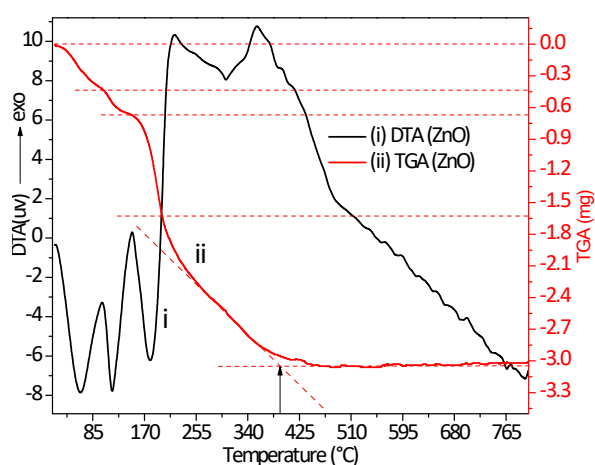


Fig. S1 Thermal gravimetric analysis and differential thermal analysis (TGA-DTA) analysis for zinc oxide (ZnO) precursor-plant extract before calcination. The total plant decomposition was observed at about 420 °C.

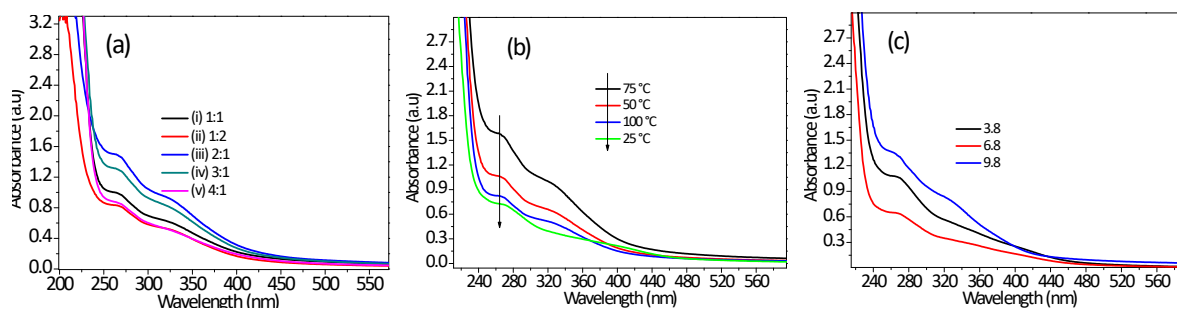


Fig. S2 The UV-vis spectra for the optimization of parameters during synthesis: (a) plant extract-precursor concentration ratio, (b) temperature, (c) pH of the solutions. The 2:1 precursor plant extract ratio, temperature of 75 °C, and pH of 9.8 were obtained as optimal conditions.

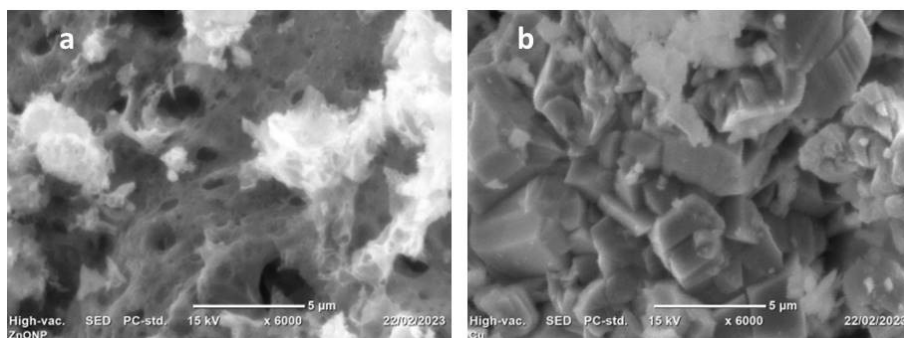


Fig. S3 SEM images (x6000) for (a) ZnO and (b) CuO, ZnO has a porous morphology and CuO has a highly crystalline morphology.

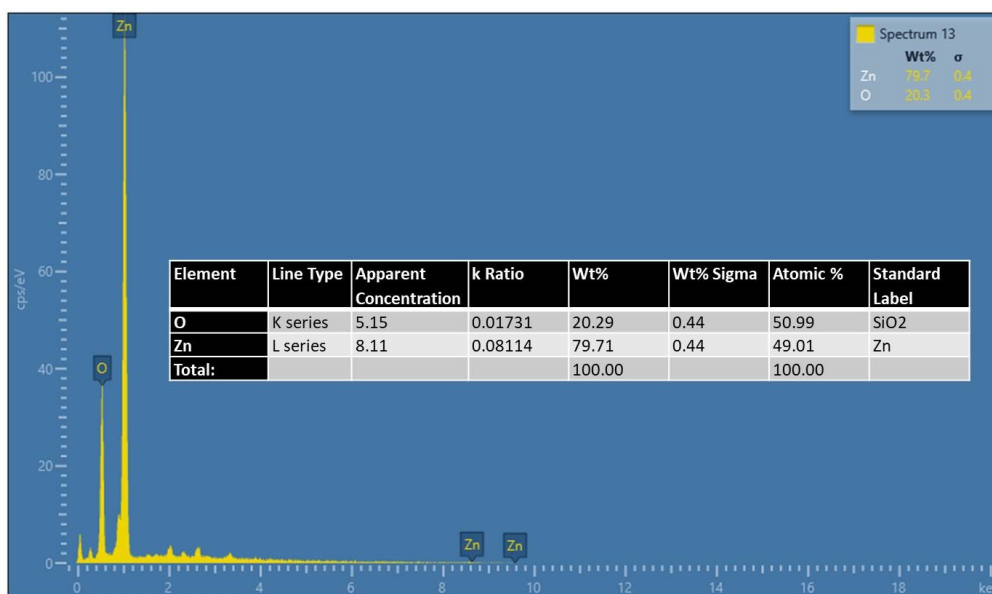


Fig. S4 EDX analysis spectrum for ZnO: The inset table show compositional analysis table; the expected elements of zinc and oxygen are detected without any impurities, confirming the ability of the method to synthesize pure material.

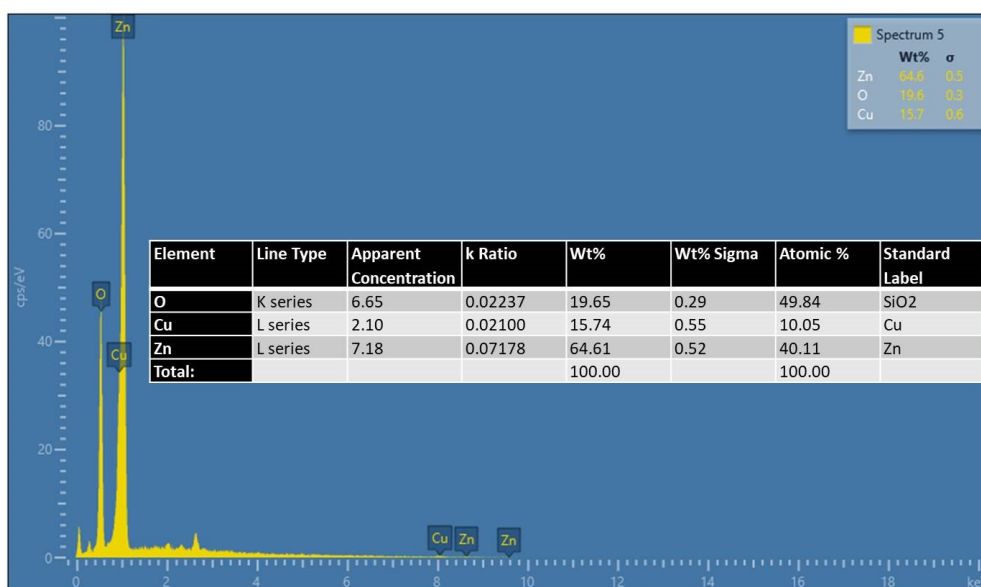


Fig. S5 EDX analysis spectrum for GCD-Z10.5; the inset table show compositional analysis table; the expected elements of zinc, copper, and oxygen are detected without any impurities, confirming the ability of the method to synthesize pure material. The obtained amounts were in accordance with the amounts added during synthesis.

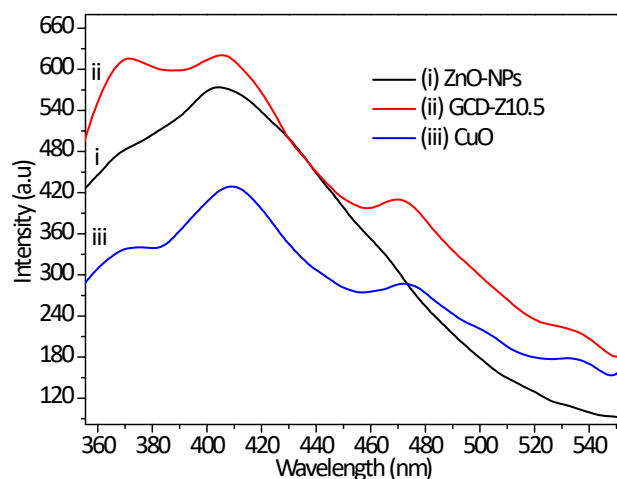


Figure S6. Optical analysis for CuO and ZnO NPs and GCD-Z10.5 NCs by the photoluminescence spectroscopic technique: Single ZnO showed a characteristic emission peak at 403 nm. Copper has three emission peaks attributed to defects: violet and green emissions. The copper emission peaks were also detected on the composite spectra, indicating the presence of CuO-ZnO local contact within the composites.

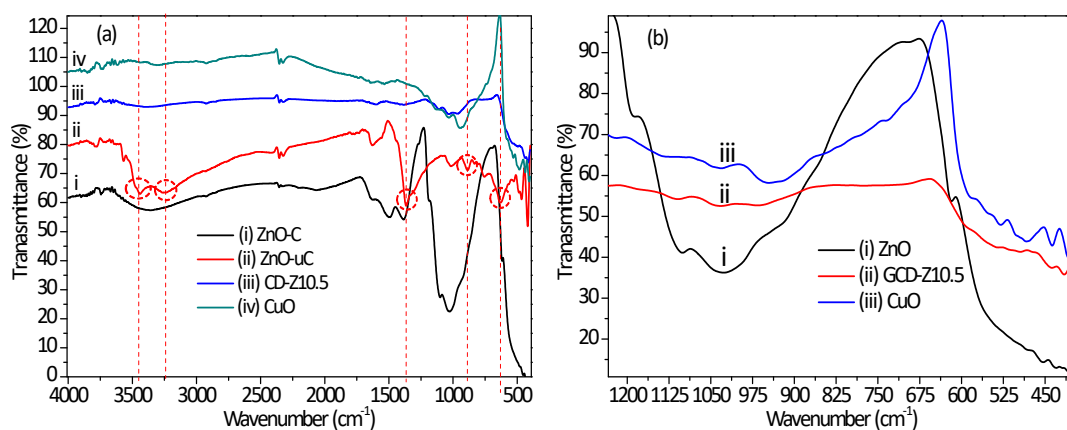


Fig. S7 Chemical bonding analysis by FTIR spectroscopic technique: (a) FTIR spectra of ZnO before and after calcination; (b) Magnified view of calcined ZnO, GCD-Z10.5, and CuO.

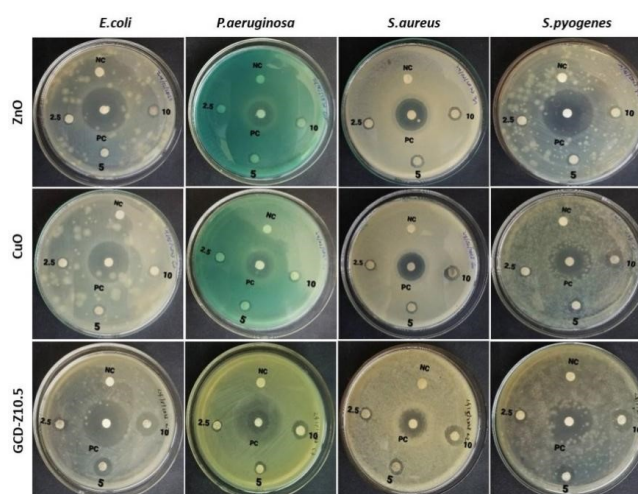


Fig. S8 Antibacterial activity determined by disc diffusion assay. Gram-negative bacteria (*E. coli* and *P. aeruginosa*) and gram-positive bacteria (*S. aureus* and *S. pyogenes*) were incubated with various concentrations of ZnO, CuO and GCD-Z10.5. The inhibition of growth of bacteria was observed around the discs and measured. The numbers on the plates indicate concentration of respective samples (2.5, 5 and 10 mg/mL), NC is negative control and PC is positive control (Chloramphenicol). GNCs (GCD-Z10.5) showed higher activity, which is plausibly due to the synergistic effect of copper and zinc. All experiments were done in triplicates.

Table S1. The precursor- extract concentration ratio, temperature, and pH optimizations: the 2:1 precursor plant extract ratio, temperature of 75 °C, and pH of 9.8 were obtained to be the optimal conditions.

Precursor:extract ratio		Temperature	pH
Precursor (mL)	extract (mL)		
10	10	25	3.8
10	20	50	6.8
*20	10	*75	*9.8
30	10	100	
40	10		

*2:1 precursor;extract ratio, 75 °C temperature, and pH of 9.8 were obtained to be optimum

Table S2. Visual observation of minimum inhibitory concentration (MIC)

GNPs & GNCs	Concentration (mg/mL)	Visual observation for bacterial growth as turbid			
		<i>S. aureus</i>	<i>E. coli</i>	<i>S. pyogenes</i>	<i>P. aeruginosa</i>
ZnO	20	Not turbid	Not turbid	Not turbid	Not turbid
	10	Not turbid	Not turbid	Not turbid	Not turbid
	5	Not turbid	Not turbid	Not turbid	Turbid
	2.5	Turbid	Not turbid	Not turbid	Turbid
	1.25	Turbid	Turbid	Turbid	Turbid
	0.625	Turbid	Turbid	Turbid	Turbid
CuO	20	Not turbid	Not turbid	Not turbid	Not turbid
	10	Not turbid	Not turbid	Not turbid	Not turbid
	5	Not turbid	Not turbid	Not turbid	Not turbid
	2.5	Not turbid	Turbid	Turbid	Turbid
	1.25	Turbid	Turbid	Turbid	Turbid
	0.625	Turbid	Turbid	Turbid	Turbid
GCD-Z10.5	20	Not turbid	Not turbid	Not turbid	Not turbid
	10	Not turbid	Not turbid	Not turbid	Not turbid
	5	Not turbid	Not turbid	Not turbid	Not turbid
	2.5	Not turbid	Not turbid	Not turbid	Not turbid
	1.25	Not turbid	Not turbid	Not turbid	Turbid
	0.625	Turbid	Turbid	Turbid	Turbid

Table S3. Minimum inhibitory concentration (MIC) of GNPs and GCD-Z10.5 based on absorbance at 600 nm.

GNPs and GNCs	Conc. (mg/mL)	Absorbance (UV) of bacterial growth before and after incubation							
		<i>S. aureus</i>		<i>E. coli</i>		<i>S. pyogenes</i>		<i>P. aeruginosa</i>	
		Before	After	Before	After	Before	After	Before	After
ZnO	20	0.068	0.064	0.078	0.069	0.068	0.060	0.074	0.061
	10	0.063	0.060	0.065	0.049	0.059	0.047	0.069	0.069
	5	0.056	0.043	0.068	0.060	0.049	0.051	0.068	0.060
	2.5	0.042	0.048	0.058	0.062	0.049	0.059	0.061	0.552
	1.25	0.044	0.315	0.052	0.148	0.041	0.213	0.060	0.623
	0.625	0.038	0.647	0.052	0.217	0.042	0.418	0.057	0.654
CuO	20	0.082	0.080	0.093	0.073	0.087	0.087	0.083	0.079
	10	0.081	0.081	0.090	0.072	0.082	0.081	0.079	0.079
	5	0.074	0.075	0.080	0.048	0.080	0.078	0.073	0.072
	2.5	0.073	0.080	0.054	0.176	0.077	0.188	0.065	0.157
	1.25	0.055	0.578	0.054	0.382	0.076	0.219	0.058	0.153
	0.625	0.045	0.674	0.040	0.382	0.074	0.488	0.049	0.319
GCD-Z10.5	20	0.081	0.074	0.081	0.080	0.084	0.080	0.085	0.079
	10	0.078	0.073	0.080	0.080	0.081	0.081	0.084	0.079
	5	0.069	0.069	0.074	0.059	0.076	0.073	0.075	0.072
	2.5	0.052	0.045	0.068	0.051	0.076	0.074	0.074	0.074
	1.25	0.048	0.085	0.053	0.051	0.074	0.074	0.067	0.153
	0.625	0.042	0.516	0.053	0.398	0.070	0.382	0.060	0.319

The highlighted values indicate the MIC of respective GNPs and GNC.

Table S4. The MIC, MBC, and TV of various GNPs and GNCs against different bacterial strains

Bacterial strains tested	MIC and MBC (mg/ml) of green synthesized nanoparticles and nanocomposite								
	ZnO			CuO			GCD-Z10.5		
	MIC	MBC	TV	MIC	MBC	TV	MIC	MBC	TV
<i>E.coli</i>	2.5	10	4	5	5	2	1.25	2.5	2
<i>P.aeruginosa</i>	5	20	4	5	20	2	2.5	5	2
<i>S.aureus</i>	2.5	10	4	2.5	5	2	1.25	2.5	2
<i>S.pyogenes</i>	2.5	10	4	5	10	4	1.25	2.5	2

Table S5. DPPH scavenging activity of GNPs, GCD-Z10.5, and ascorbic acid (vitamin C).

[] ^a (µg/mL)	AA ^b		ZnO		CuO		GCD-Z10.5	
	(Abs) ^c	% RSA ^d	(Abs)	% RSA	(Abs)	% RSA	(Abs)	% RSA
2000	0.101	93.3	0.689	54.4	0.625	58.6	0.462	69.4
1000	0.108	92.8	0.821	45.6	0.712	52.8	0.542	64.1
500	0.113	92.5	1.033	31.6	0.995	34.1	0.714	52.7
250	0.128	91.5	1.112	26.4	1.114	26.2	0.881	41.6
125	0.138	90.8	1.136	24.8	1.124	25.6	1.002	33.6
Control (4%) ^e	1.51	0	1.51	0	1.51	0	1.51	0

^a is concentration; ^b is ascorbic acid (standard control); ^c is Absorbance; ^d is %radical scavenging activity; ^e is absorbance of DPPH alone at the concentration of 4mg/100mL.

References

- 1 S. Hayat, A. Ashraf, M. Zubair, B. Aslam, M. H. Siddique, M. Khurshid, M. Saqalein, A. M. Khan, A. Almatroudi, Z. Naeem and S. Muzammil, *PLoS One*, 2022, **17**, e0259190.
- 2 D. B. Sbhathu and H. B. Abraha, *Evidence-Based Complement. Altern. Med.*, 2020, **2020**, 1–6.
- 3 D. M. Musyimi, T. A. Ashioya, G. Opande and W. O. Emitaro, *Bact. Emp.*, 2021, **4**, e183.
- 4 K. N. Agbafor and N. Nwachukwu, *Biochem. Res. Int.*, 2011, **2011**, 1–4.
- 5 B. Oloya, J. Namukobe, W. Ssenkooba, M. Afayoa and R. Byamukama, *Trop. Med. Health*, 2022, **50**, 16.
- 6 M. G. Agidew, *Bull. Natl. Res. Cent.*, 2022, **46**, 87.
- 7 R. Hussain, A. Zafar, M. Hasan, T. Tariq, M. S. Saif, M. Waqas, F. Tariq, M. Anum, S. I. Anjum and X. Shu, *Appl. Biochem. Biotechnol.*, 2023, **195**, 264–282.